BNL-99276-2013-TECH

C-A/AP/124;BNL-99276-2013-IR

Analysis from Beam Studies with BTA Stripping Foils

G. Marr

November 2003

Collider Accelerator Department

Brookhaven National Laboratory

U.S. Department of Energy

USDOE Office of Science (SC)

DISCLAIMER

C-A/AP/#124
November 2003

Analysis from Beam Studies with BTA Stripping Foils

G. Marr, L. Ahrens, P. Thieberger, K. Zeno

Collider-Accelerator Department
Brookhaven National Laboratory
Upton, NY 11973

Analysis from Beam Studies with BTA Stripping Foils

G. Marr, L. Ahrens, P. Thieberger, K. Zeno

1. Introduction

Prior to the FY 2003 Gold-Deuteron run for RHIC, a number of stripping foils in the BTA transport line apparatus were exchanged with new foils. A variety of materials and thickness have been used, as summarized in Table 1, along with the set of foils to be installed for FY '04; beam measurements at the Tandem Van de Graaf were used to calculate thickness [1, 2]. Note that Carbon foil #4 has been the foil of choice for typical beam operations. The purpose for employing new foils was primarily to reduce momentum spread in the Gold beam entering the AGS. Foil stripping efficiency was also an important consideration, in terms of obtaining a favorable charge state distribution for the desired charge state (Au^{77+}); maintaining transverse beam size was also considered.

Foil	Prior to FY '03		FY '03		Proposed FY '04	
#	**Material**	**Thickness**	**Material**	**Thickness**	**Material**	**Thickness**
1	Blank position	mg/cm^2				
2	Carbon .003"	13.9*	Carbon .003"	14.2	*(Unchanged)*	
3	Carbon .004"	18.5*	*(Unchanged)*	20.6	Beryllium .005"	23.2
4	Carbon .005"	23.1*	*(Unchanged)*	23.1*	*(Unchanged)*	
5	Carbon .007"	32.4*	Carbon .0052"	24.2	*(Unchanged)*	
6	Carbon .010"	46.2*	Mica	25.8	Beryllium .006"	28.3
7	Copper .001"	22.8*	Titanium .00276"	29.9	Silica .005"	27.7
8	Carbon/Copper .001/.003"	22.8/13.9*	Silica .0041"	22.5	*(Unchanged)*	

Table 1: Recent history of foil configurations (denotes calculated estimates rather than beam measurements)*

2. Momentum Spread

To measure the momentum spread of the beam, studies utilized a mountain-range display of the AGS B4 pick-up electrode to view the 6 Booster bunches as they are injected into the AGS. In this case, AGS RF voltage was disabled, allowing the beam to debunch. From the mountain range display, a measurement of the beam revolution frequency can be determined. Combined with a measurement of Booster beam frequency at extraction, the change in frequency Δf can be calculated; energy loss from passing through the foil is then calculated employing the equations

$$\beta = \frac{2\pi R_I f}{c} \text{ and } W = mc^2(\gamma - 1),$$

where $R_I = 128.4526$ meters is the nominal AGS radius at injection [3]. Furthermore, one can interpret the mountain-range display to calculate the number of turns required for the overlap of low-momentum particles in the last injected bunch with high-momentum particles from first bunch injected; the inverse of which provides $\Delta f / f$. Momentum spread is then calculated using the relation

$$\frac{\Delta\tau}{\tau} = \eta\frac{\Delta p}{p} = \frac{\eta}{\beta^2}\frac{\Delta E}{E},$$

where the slip factor η is defined as

$$\eta = \frac{1}{\gamma_T^2} - \frac{1}{\gamma^2} \text{ [4].}$$

Measurements of these parameters are summarized in Table 2. Figures 1 and 2 show measured energy loss due to the foil and momentum spread, respectively.

Foil #	Material	df (MHz) 17-Oct	df (MHz) 3-Nov	dW (MeV/N) 17-Oct	dW (MeV/N) 3-Nov	dp/p
4	Carbon .005"	0.0618	0.0619	3.733	3.736	0.00625
6	Mica		0.0722		4.348	0.00125
7	Titanium	0.0750	0.0765	4.518	4.602	0.001666667
8	Silica	0.0652	0.0660	3.936	3.980	0.001923077

Table 2: Measured energy loss and momentum spread

3. Charge State Distribution/Stripping Efficiency

A number of methods were used to determine efficiency through the stripping foil and charge state distribution. In the BTA line, there are multiwires at 6’ and 60’ in the line (designated MW006 and MW060, respectively), upstream and downstream of the stripping foil. Figure 3 shows an example of a multiwire profile. Since the beam is bent horizontally between the foil and MW060, the horizontal profile can be used to view multiple charge states, and the voltage on the wires (in combination with those of MW006) can determine the relative beam intensity. Table 3 summarizes these results. The profile peak amplitudes between charge states 77^+ and 76^+ are plotted in Figure 4, showing the consistency between the data taken in November 2002 and March 2003. Figure 5 plots the efficiency through the foil for the desired charge state. Both indicate our highest yield of charge state 77^+ was obtained with foil 5. By summing the wires for the various charge states it was possible to estimate the distribution mean charge. Four Booster cycles of data with beam were summed, and a fifth cycle of data without beam used for a background subtraction. The horizontal magnet DH2-3 (between the foil and MW060) was adjusted in order to view additional charge states. These summed profiles are shown in Figures 6-9. In the instances where the charge state profile approaches the edge of the multiwire, the missing values were estimated from the opposite side of the charge distribution. The relative abundances of the various charge states for four foils are displayed in Figure 10.

Foil #	Material	Multiwire voltage ratio 3-Nov	$77^+/76^+$ peak ratio		Distribution mean charge 19, 23-Mar
			3-Nov	19, 23-Mar	
2	Carbon .003”	0.387207457			
3	Carbon .004”	0.381790744	2.432098765		
4	Carbon .005”	0.41980834	2.714285714	2.50714	76.78
5	Carbon .0051”	0.439610965	3.144329897		
6	Mica	0.297763254	1.884615385	1.97179	76.71
7	Titanium	0.17476638	0.934579439	1.086064	76.11
8	Silica	0.366249433	2.12345679	2.089645	76.75

Table 3: Measured multiwire profile data

4. Transverse Emittance

With the multiwire data (utilized in Section 3), it is also possible to evaluate the relative changes in transverse emittance due to the various foils. In this case, the central beam profile (Au^{32+} upstream of the foil, Au^{77+} downstream) wire voltages were used to create a crude estimate of the Gaussian full-width at half-maximum; the results are plotted in Figure 11. The carbon foil data validate the reasonable assumption that thinner foils of the same material cause less transverse beam growth. Multiple Coulomb scattering angles for the various foils were calculated using known radiation length data [5] and the approximation

$$\theta_{\circ} = \frac{13.6MeV}{\beta cp} Z \sqrt{\frac{x}{X_{\circ}}} \left(1 + 0.038 \ln \frac{x}{X_{\circ}} \right)$$

where β, p, Z refer to the incident particle and $x, X_{\circ}$ are the foil's thickness and radiation length, respectively [6]. The correlation of scattering angle (also plotted in Figure 11) with the emittance growth through the foil is unclear.

5. Conclusions

The new foils in place for FY '03 showed promise in reducing momentum spread in the AGS as compared to Carbon. However, Carbon foils still produce greater efficiency for the injected charge state, Au^{77+}. The new materials installed for FY '04 will further investigate this space to improve our transmission efficiency while providing low momentum spread. The charge state distribution data collected in these studies could be further analyzed to determine absolute cross sections.

References

1. C.J. Gardner, "New Foils in the BTA Line", Booster/AGS Setup Logbook AG.303.2.0301, September 13, 2002, pp. 56-59.
2. P. Thieberger, private communication.
3. L.A. Ahrens and C.J. Gardner, "Calculation of the Mean Energy Loss in the BTA Stripping Foils and Comparison with Measurement", CA/AP Note No. 76, July 1, 2002.
4. E.D. Courant and H.S. Snyder, "Theory of the Alternating Gradient Synchrotron", Annals of Physics 3, 38 (1958).
5. K. Hagiwara et al., "Review of Particle Physics", Physics Letters D 66, 1 (2002).
6. A.W. Chao and M. Tigner, Handbook of Accelerator Physics and Engineering, World Scientific, Singapore, 1999, p. 213.

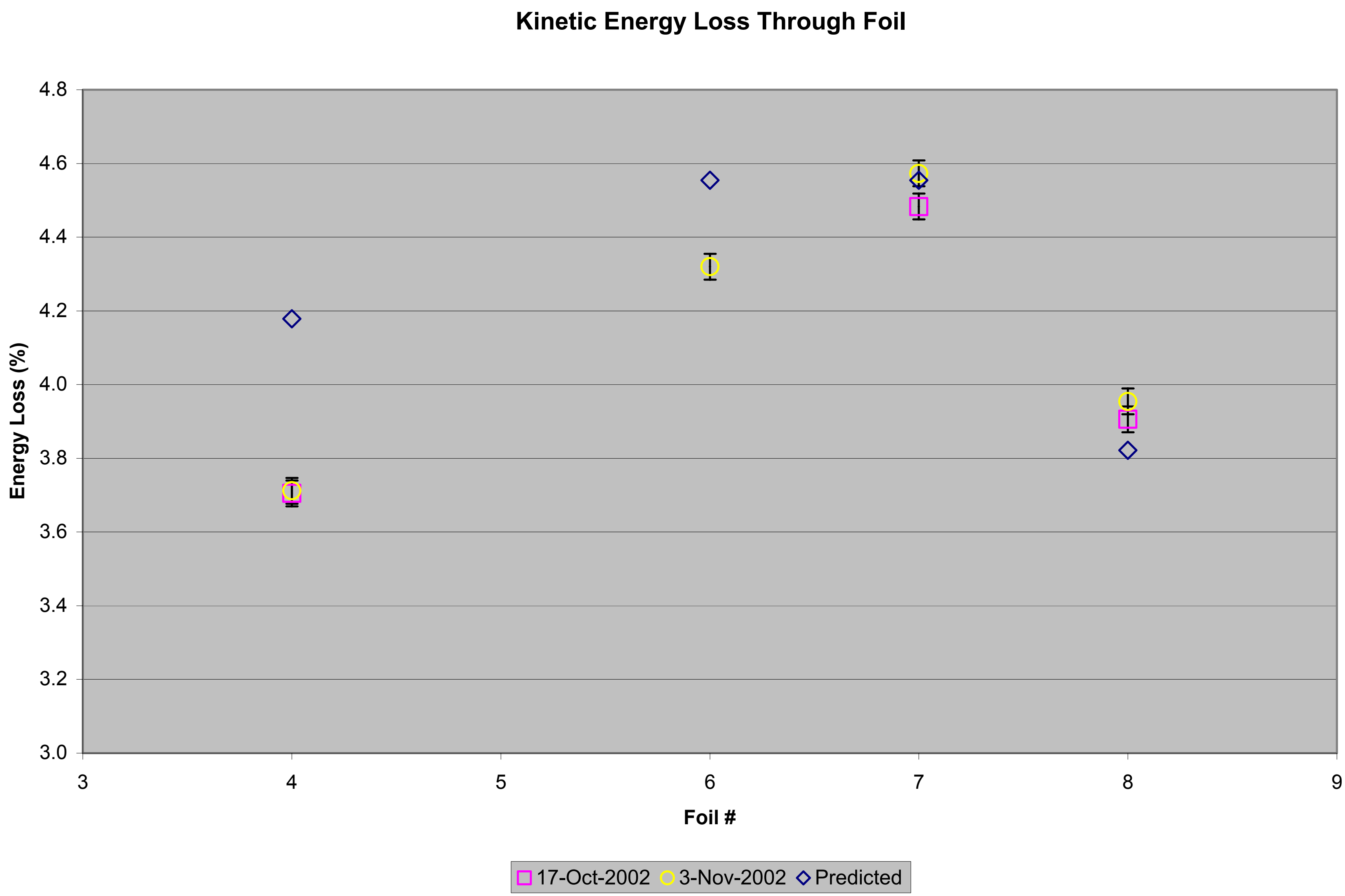

Figure 1: Energy loss due to foil

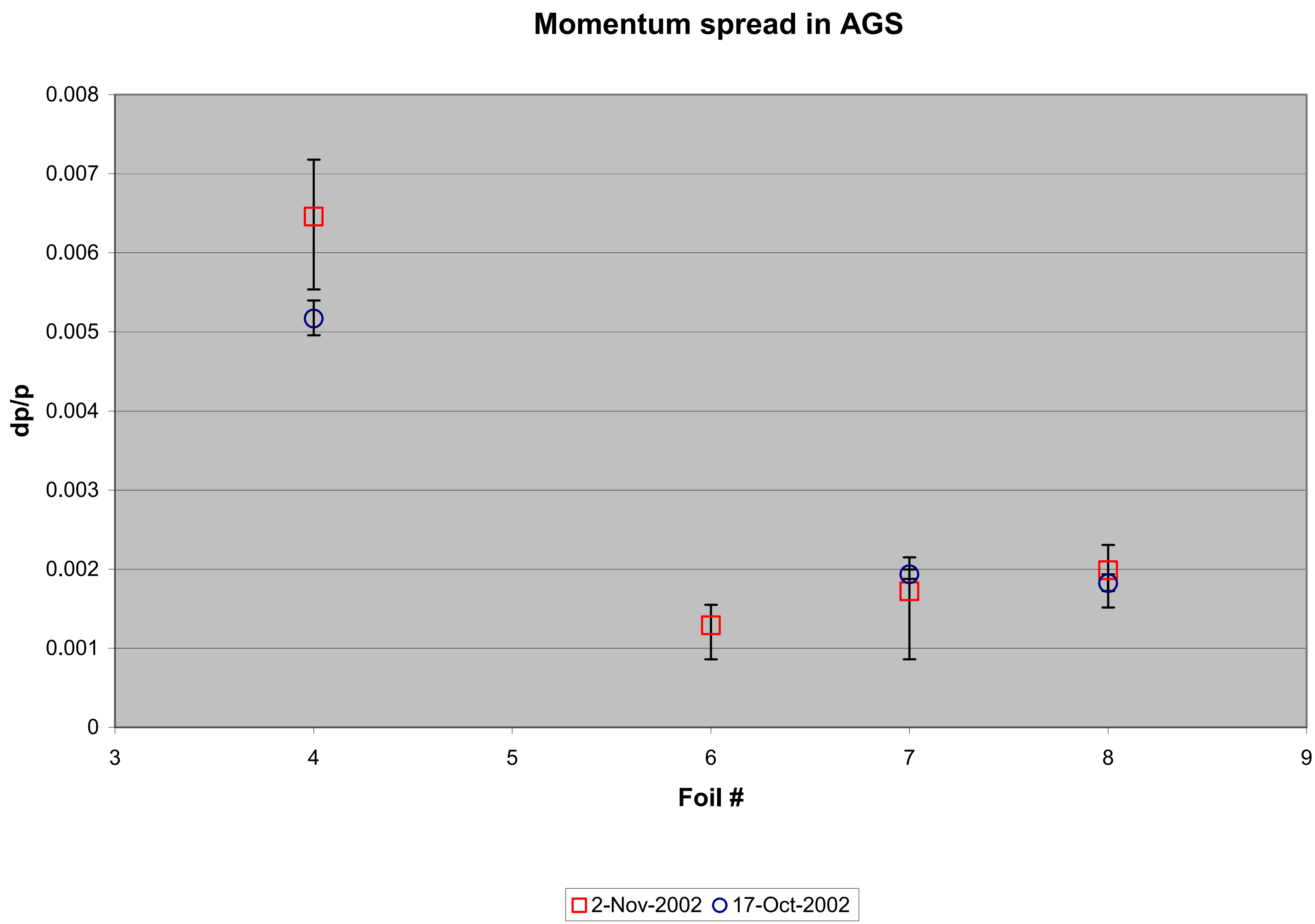

Figure 2: Measured momentum spread in AGS for various foils

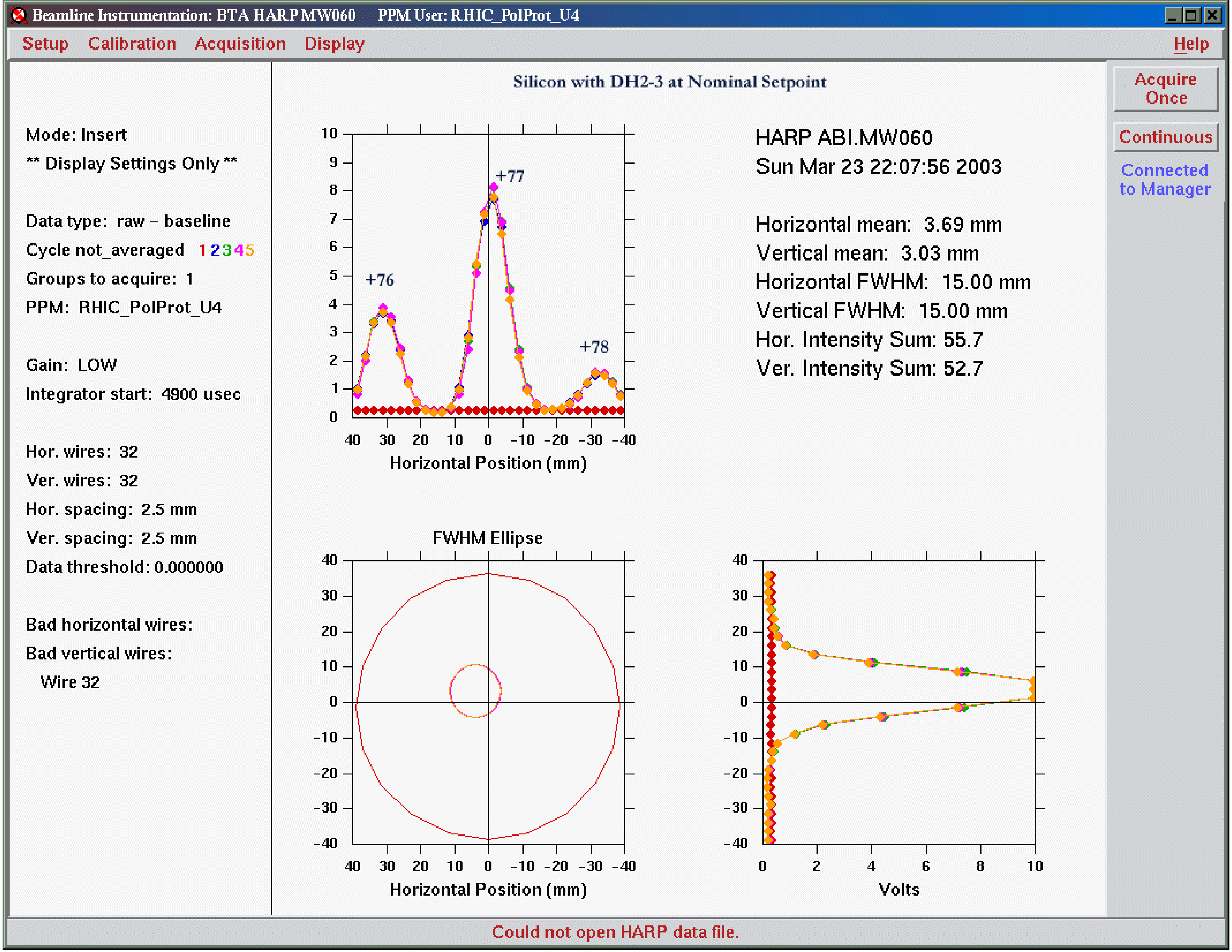

Figure 3: Typical multiwire profile, with charge states annotated

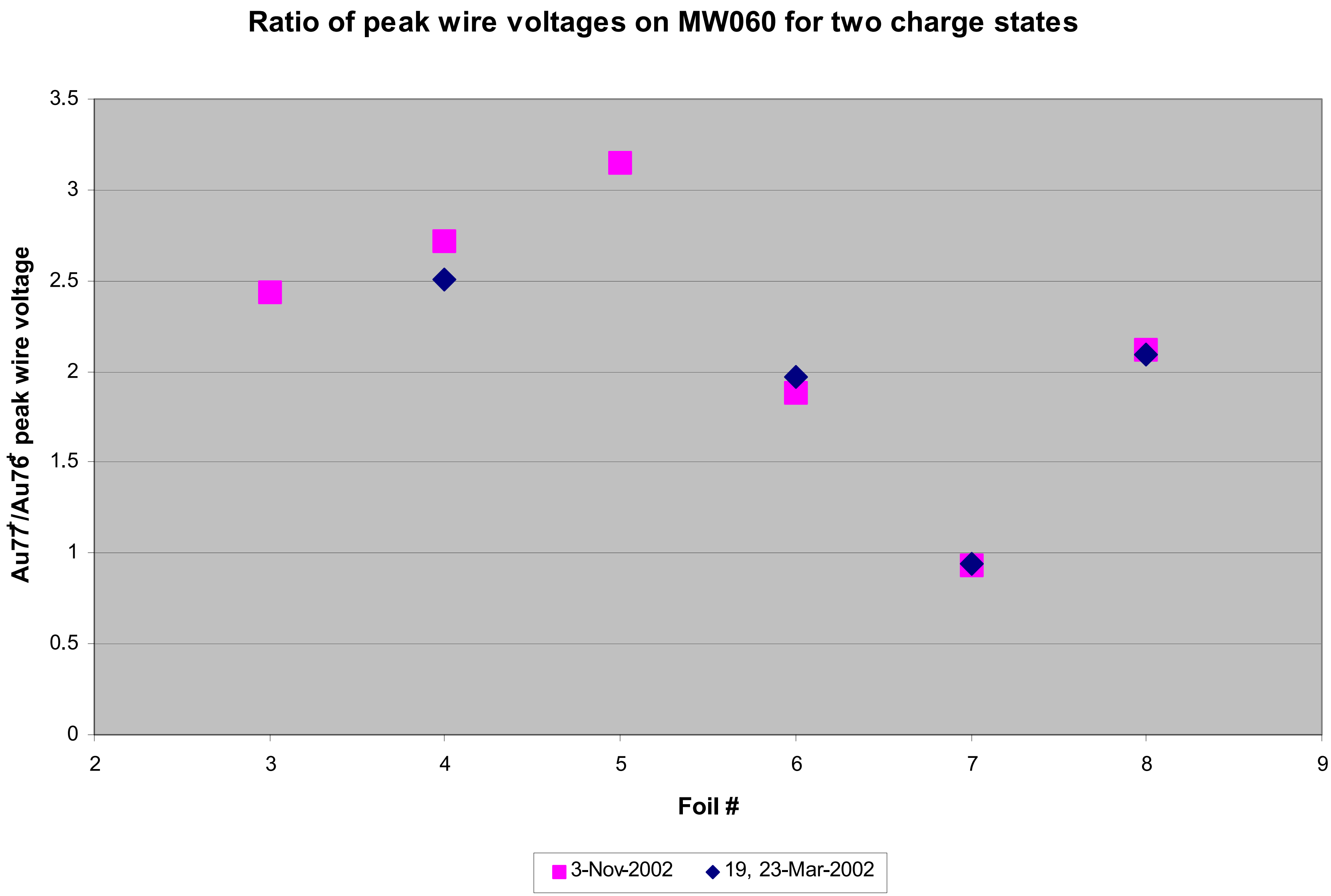

Figure 4: Comparison of charge distribution data

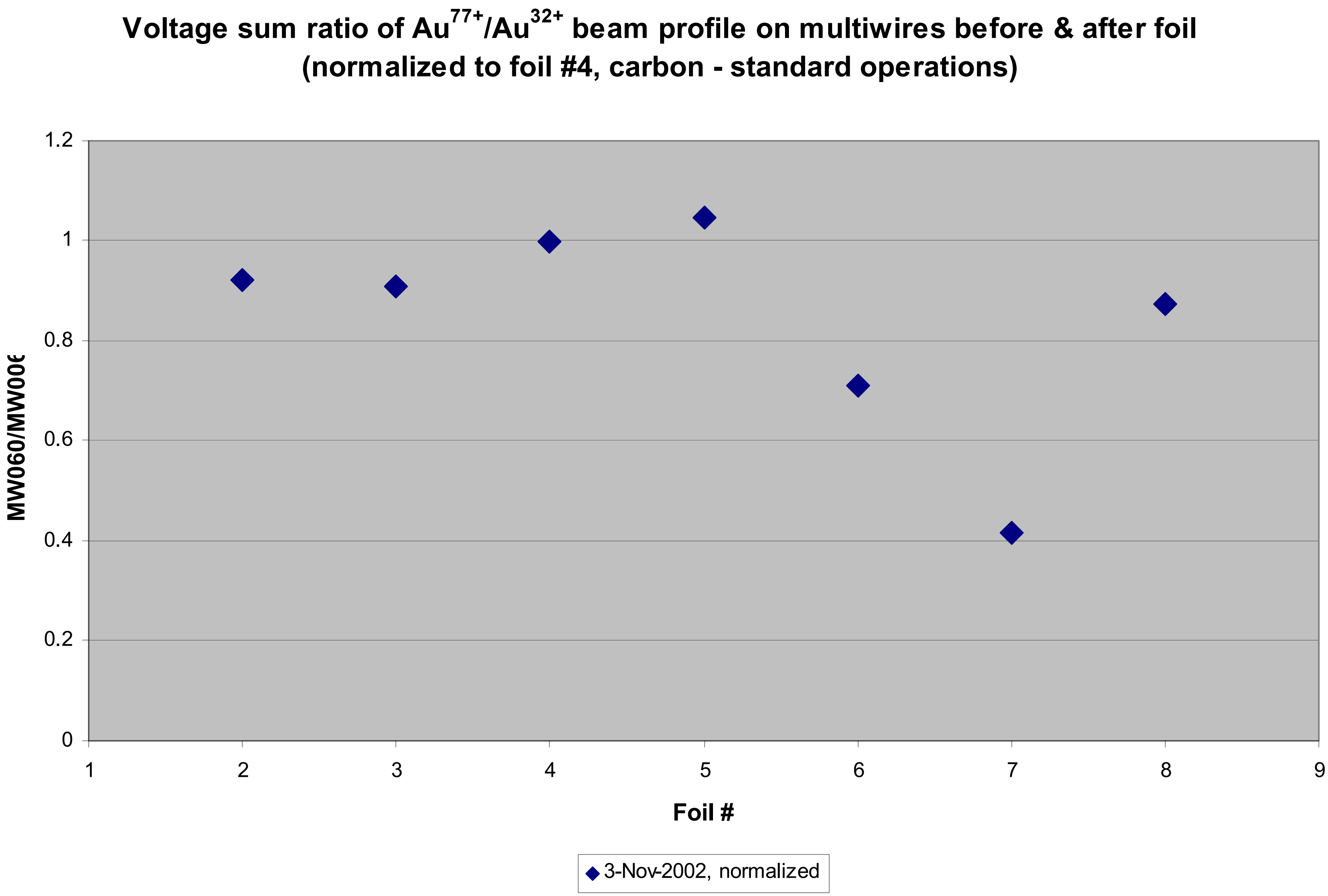

Figure 5: Transmission of desired charge state through foil

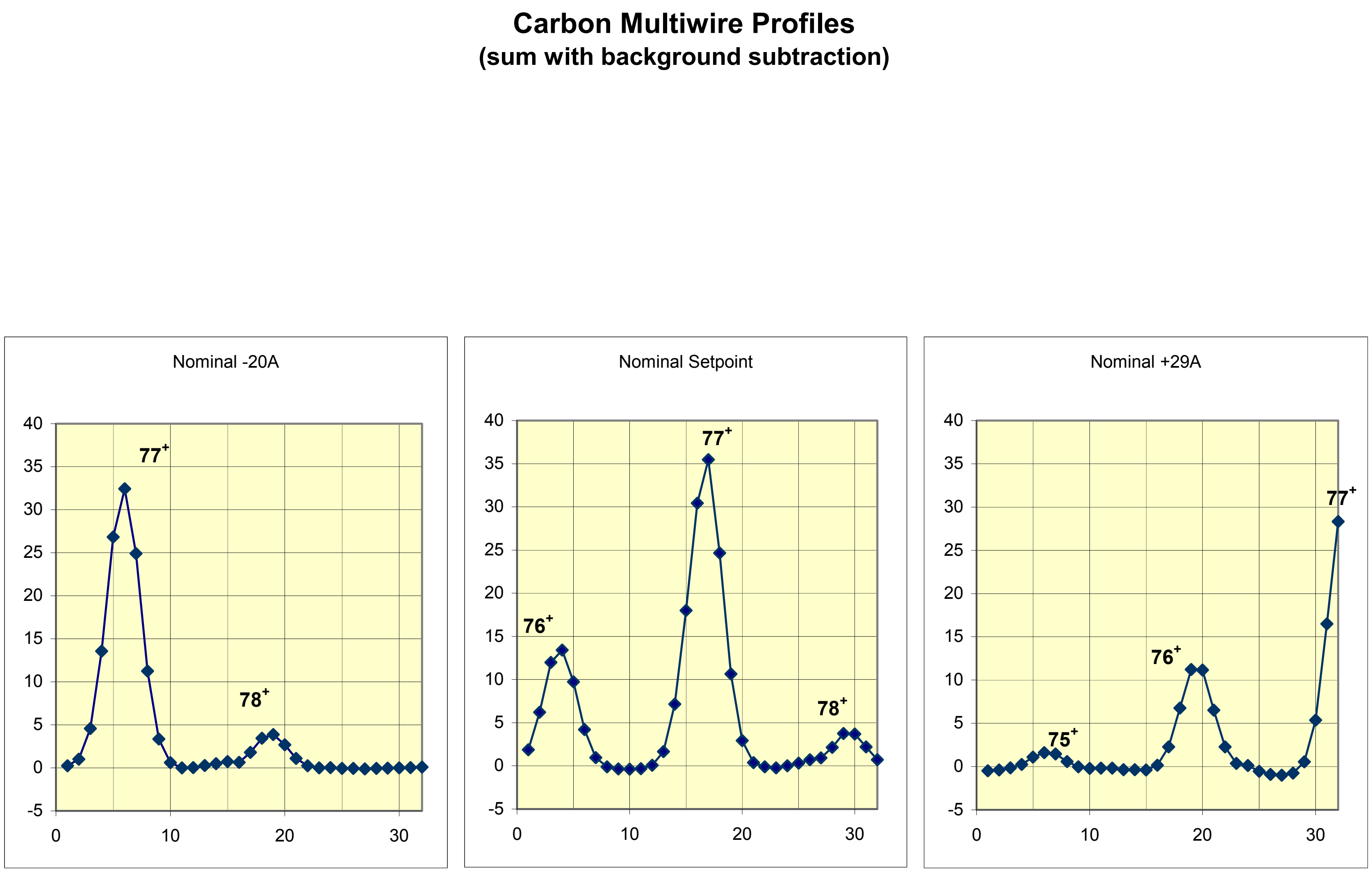

Figure 6: Profiles at MW060 with carbon foil (#4)

Mica Multiwire Profiles
(sum with background subtraction)

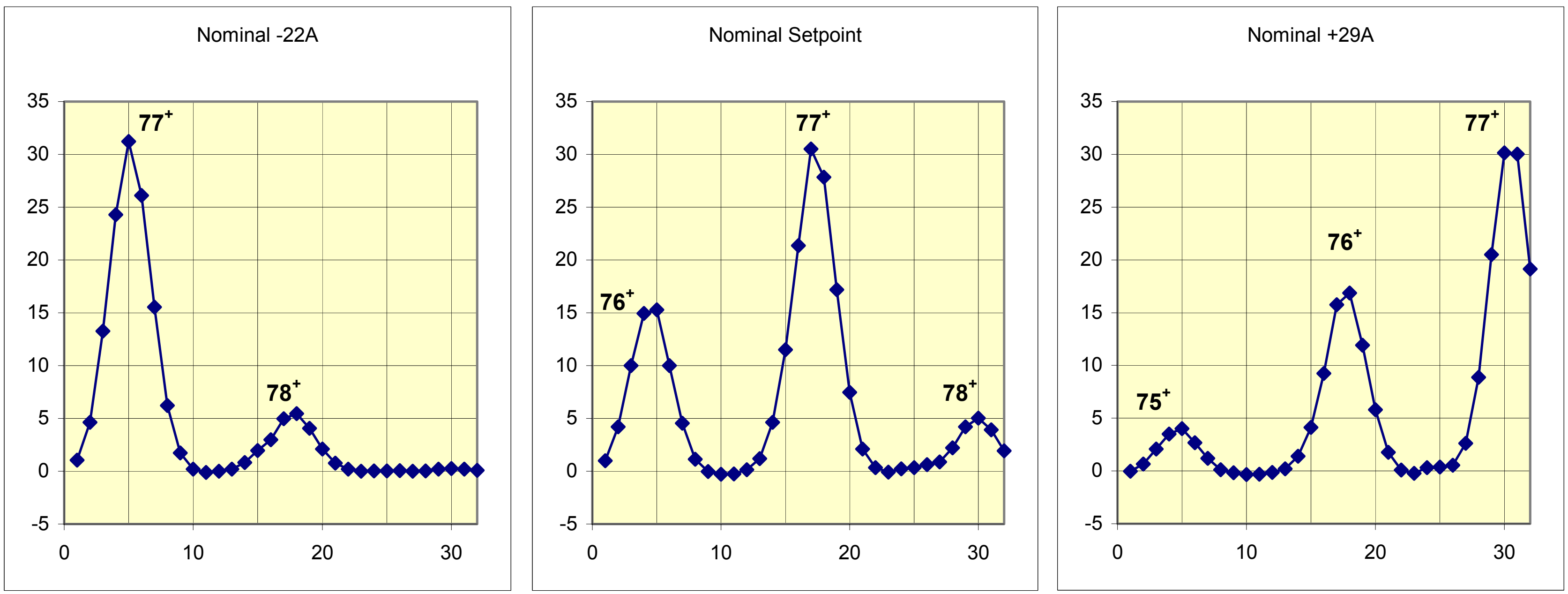

Figure 7: Profiles at MW060 with mica foil

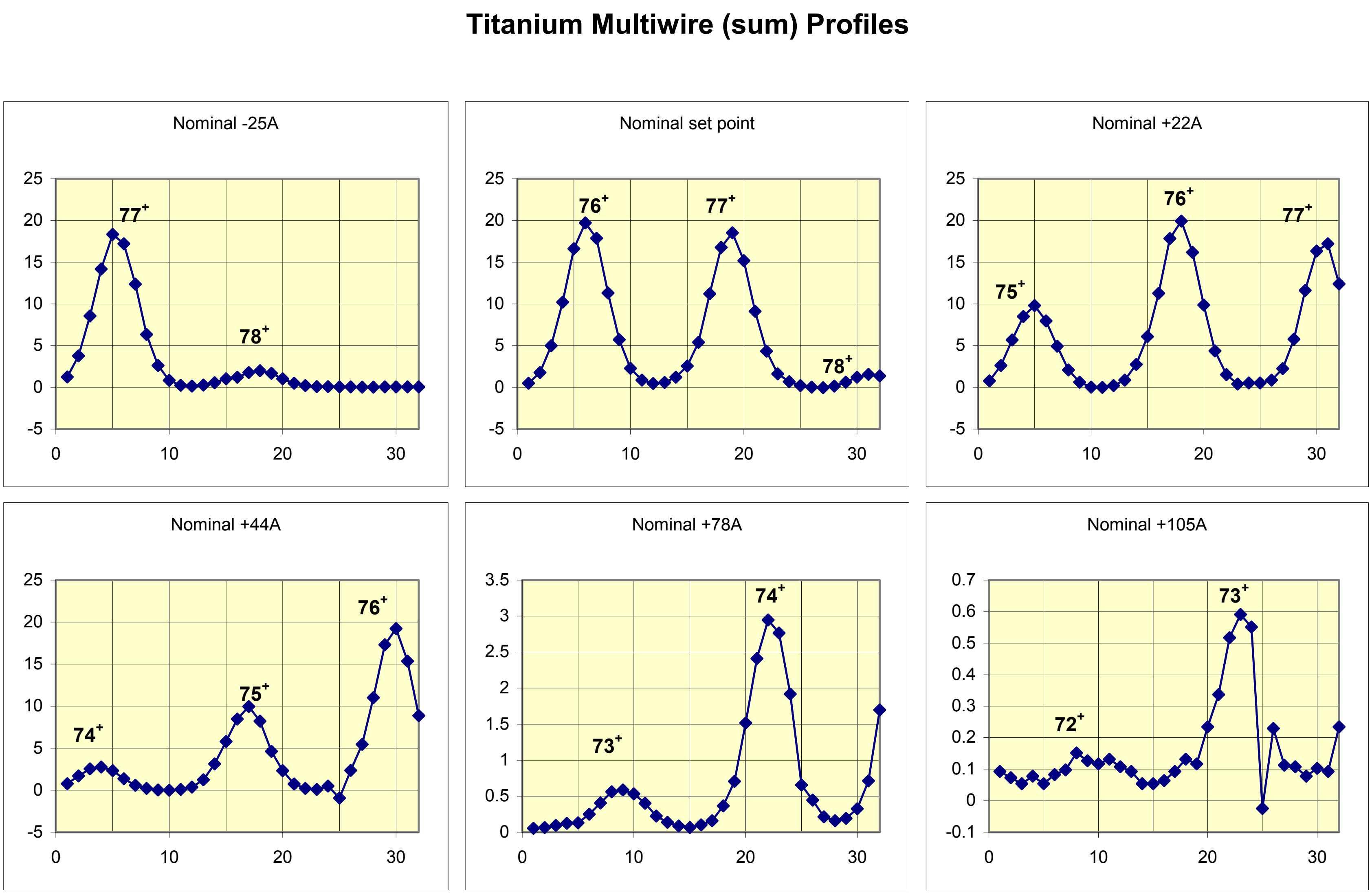

Figure 8: Profiles at MW060 with titanium foil

Silica Multiwire (sum) Profiles

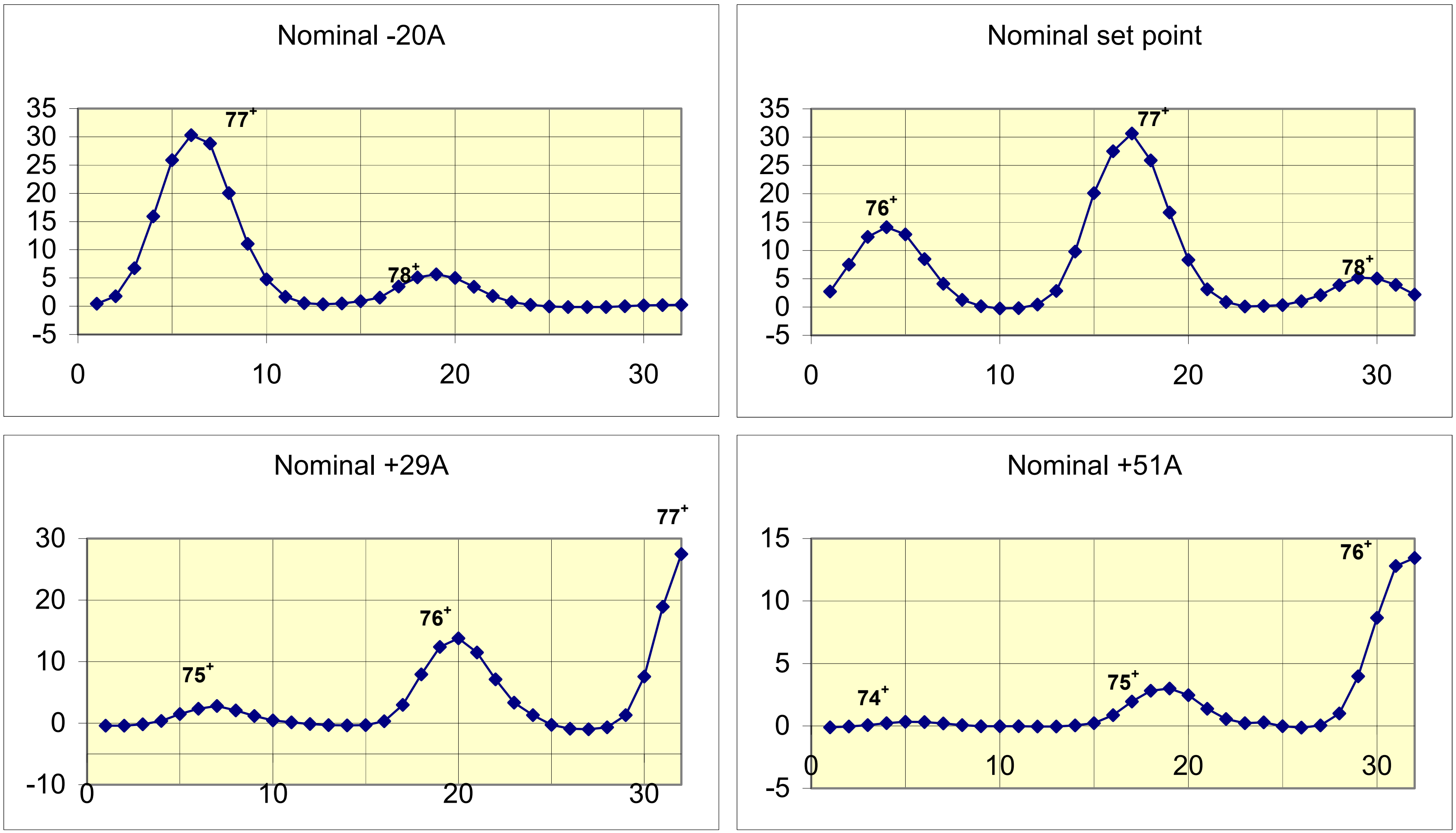

Figure 9: Profiles at MW060 with silica foil

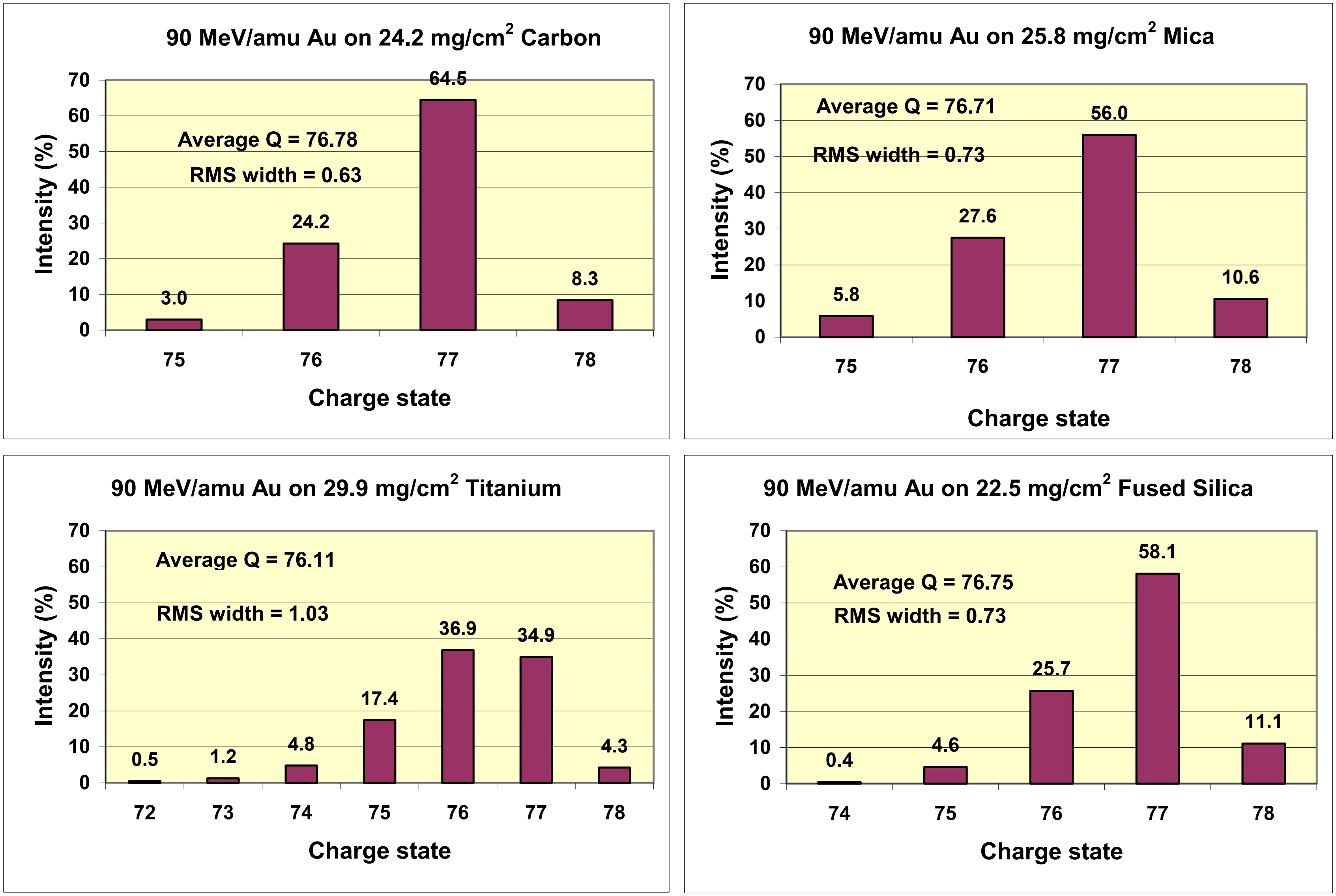

Figure 10: Charge distributions

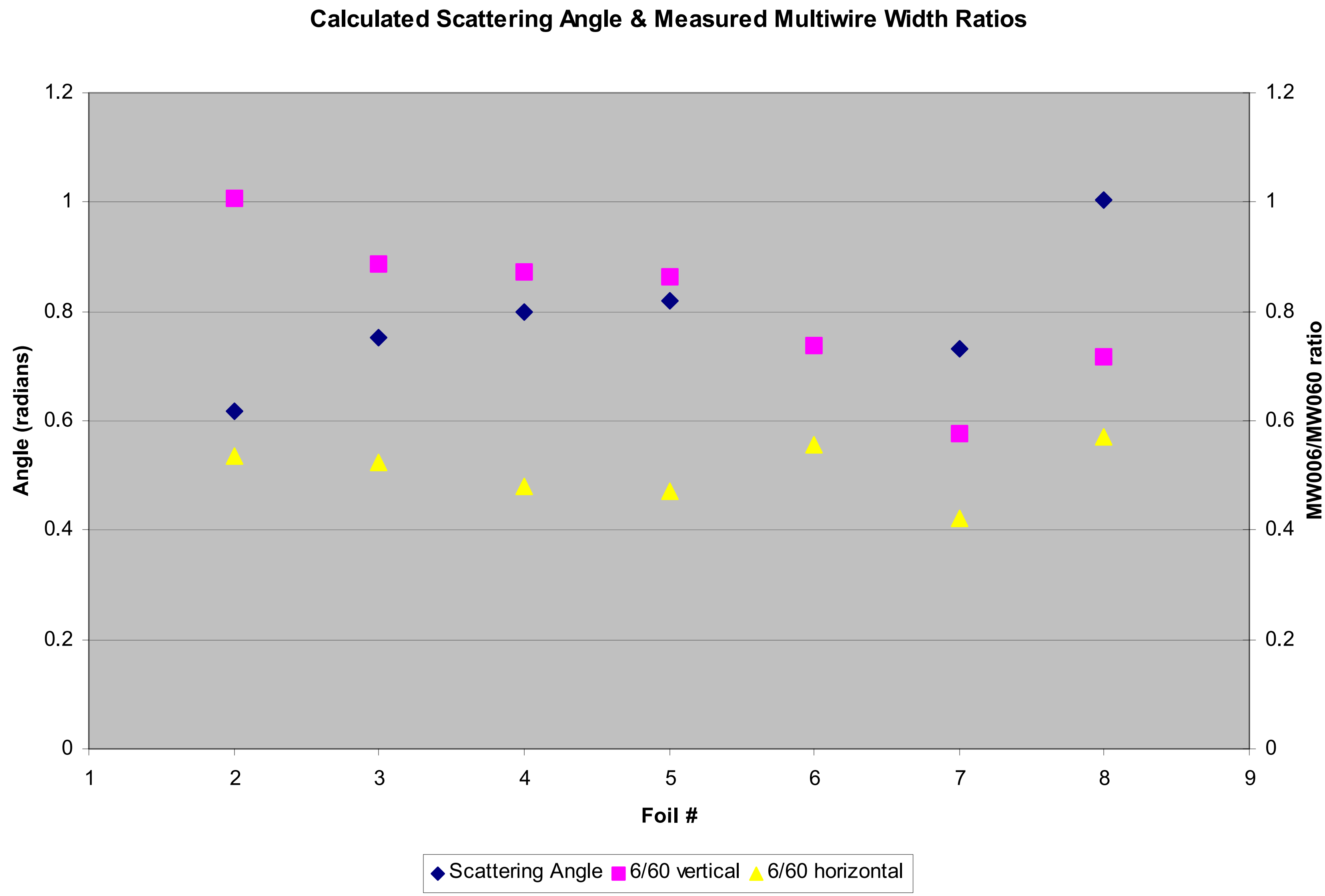

Figure 11: Transverse emittance estimate ratios compared to scattering angle calculations